Thermal Conductivity and Thermal Expansivity of Thermotropic Liquid Crystalline Polymers

C. L. CHOY,[1]* Y. W. WONG,[1] K. W. E. LAU,[1] GUANGWU YANG,[1] and A. F. YEE[2]

Department of Applied Physics and Materials Research Centre, The Hong Kong Polytechnic University, Hung Hom, Kowloon, Hong Kong; Department of Materials Science and Engineering, University of Michigan, Ann Arbor, Michigan 48109

SYNOPSIS

The thermal conductivity and thermal expansivity of a thermotropic liquid crystalline copolyesteramide with draw ratio λ from 1.3 to 15 have been measured parallel and perpendicular to the draw direction from 120 to 430 K. The sharp rise in the axial thermal conductivity $K_{\parallel}$ and the drastic drop in the axial expansivity $\alpha_{\parallel}$ at low λ, and the saturation of these two quantities at $\lambda > 4$ arise from the corresponding increase in the degree of chain orientation revealed by wide-angle x-ray diffraction. In the transverse direction, the thermal conductivity and expansivity exhibit the opposite trends but the changes are relatively small. The draw ratio dependences of the thermal conductivity and expansivity agree reasonably with the predictions of the aggregate model. At high orientation, $K_{\parallel}$ of the copolyesteramide is slightly higher than that of polypropylene but one order of magnitude lower than that of polyethylene. In common with other highly oriented polymers such as the lyotropic liquid crystalline polymer, Kevlar 49, and flexible chain polymer, polyethylene, $\alpha_{\parallel}$ of the copolyesteramide is negative, with a room temperature value differing from those of Kevlar 49 and polyethylene by less than 50%. Both the axial and transverse expansivity show transitions at about 390 and 270 K, which are associated with large-scale segmental motions of the chains and local motions of the naphthalene units, respectively. © 1995 John Wiley & Sons, Inc.

Keywords: thermotropic liquid crystalline polymers • thermal conductivity • thermal expansivity • orientation function

INTRODUCTION

Thermotropic liquid crystalline polymers (TLCP) have attracted considerable recent attention because of their dimensional stability and excellent mechanical performance. When a TLCP is drawn from the melt, the elongational stress leads to the formation of a microfibrillar structure, with the microfibrils aligning along the draw direction. Because the molecular chains in the microfibrils are also highly oriented, the drawn materials have very high axial stiffness and strength.

The mechanical properties of oriented TLCP have been extensively studied.[1-6] However, there have been comparatively few reports on the effect of orientation on other technically important properties such as thermal conductivity[7,8] and thermal expansivity.[9,10] Crispin and Greig[7] studied the thermal conductivity of several highly oriented TLCP but the measurements were limited to the temperature range below 100 K. We have investigated the effect of the skin–core structure of an injection-molded TLCP by measuring the thermal conductivity as a function of position.[8] Green et al.[9] have measured the axial thermal expansivity $\alpha_{\parallel}$ of oriented TLCP from 200 to 430 K whereas Takeuchi et al.[10] have investigated the draw ratio dependence of $\alpha_{\parallel}$ for polyethylene terephthalate/*p*-oxybenzoate copolyester at room temperature. In the present work, the thermal conductivity and thermal expansivity of a liquid crystalline copolyesteramide with draw ratio from 1.3 to 15 have been measured parallel and

* To whom correspondence should be addressed.

Journal of Polymer Science: Part B: Polymer Physics, Vol. 33, 2055–2064 (1995)
 CCC 0887-6266/95/142055-10

perpendicular to the draw direction between 120 and 430 K. It is found that the axial thermal conductivity rises sharply whereas the axial expansivity drops drastically with increasing draw ratio. Like flexible chain polymers, these changes can be attributed to the increase in the degree of molecular orientation in the polymer.

EXPERIMENTAL

Sample Preparation

The starting materials are Vectra B950 and Vectra A950 produced by Hoechst-Celanese Co. Vectra B950 is a copolyesteramide consisting of 58 mol % 2,6-hydroxynaphthoic acid (HNA), 21 mol % terephthalic acid, and 21 mol % para-aminophenol and Vectra A950 is a copolyester comprising 30 mol % HNA and 70 mol % *p*-hydroxybenzoic acid (HBA). Pellets of Vectra B950 were fed into a Werner-Pfleiderer 30 mm co-rotating twin-screw extruder equipped with a 3.2-mm conical die. The downstream barrel temperatures were set at 290°C. The extruded rod was led through a set of take-up reels, and the speeds of these reels were adjusted to give rods of various diameters. The draw ratio λ is defined as the ratio of the cross-sectional area of the die to that of the drawn rod. For comparison, we have also studied an extruded rod of Vectra A950 ($\lambda = 3$) supplied by Hoechst-Celanese Co. The density ρ of all the rod samples determined by the flotation method falls in the narrow range 1.395–1.404 g/cm^3, so an average value of 1.40 g/cm^3 is used in subsequent calculations.

Wide-Angle X-Ray Diffraction

It is generally agreed[6,11] that the aperiodic meridional x-ray reflections observed in thermotropic copolyesters and copolyesteramides arise as a result of diffraction from oriented randomly substituted chains. The sharpness of these reflections gives an indication of the coherence length of the diffraction units, a value of 10 monomers being typical for these TLCP. The azimuthal intensity distribution of the strongest meridional reflection ($2\theta = 43°$ for CuKα radiation) was recorded with a Philips Xpert diffractometer equipped with a pole figure attachment. From these data we calculate the orientation function

$$f = \tfrac{1}{2}(3\,\overline{\cos^2\alpha} - 1)$$

where α is the angle between the diffracting unit and the draw direction, and the bar denotes average over all units.

Thermal Conductivity Measurements

The detailed procedure of the laser-flash radiometry technique has been reported,[12] so only a brief description is given. Films of TLCP, about 0.15 mm thick, were cut with their normals parallel or perpendicular to the draw axis and then attached to the sample holder. A laser beam of wavelength 266 nm was flashed on the front surface of the sample and the thermal radiation from the rear surface was focused by a germanium lens onto a liquid nitrogen-cooled HgCdTe infrared detector. Apertures of the same size as the sample were placed in the front and back of the sample to ensure that only the sample was irradiated by the laser beam and only the thermal radiation emitted by the sample was detected.

The signal from the detector was amplified and fed to a transient digitizer. Room temperature measurements were performed by averaging the results for 20 laser shots, but 100 shots were required to give a sufficiently good signal at 160 K. The signal as a function of time was collected by using a microprocessor and then fitted to a theoretical expression to give the thermal diffusivity D. The thermal conductivity K is calculated from the relation:

$$K = \rho C D$$

where the specific heat C was determined with an accuracy of 2% on a Perkin-Elmer DSC-7 differential scanning calorimeter. The accuracy of K is about 6%.

Thermal Expansivity Measurements

The change in the length of the samples was measured at a heating rate of 10 K/min by a Perkin-Elmer TMA-7 thermomechanical analyzer. The linear thermal expansivity, calculated by the method previously described,[13] has an accuracy of 6%.

RESULTS AND DISCUSSION

Chain Orientation

Figure 1 shows the orientation function f of the extruded TLCP rods as a function of draw ratio λ. The orientation function increases rapidly at low λ but be-

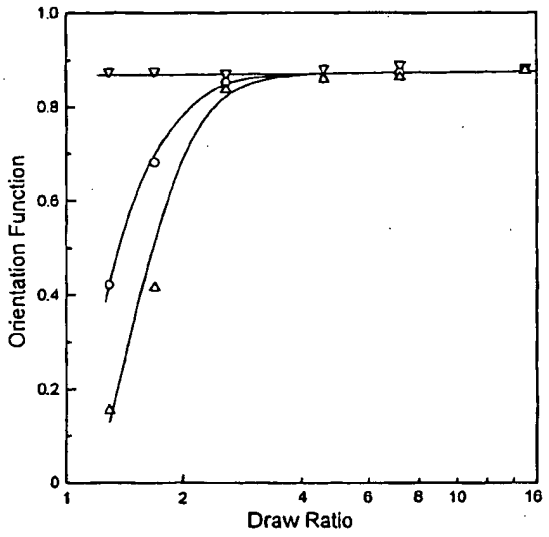

Figure 1. Draw ratio dependence of the orientation function for Vectra B950. Skin, ▽; core, △; whole rod, ○.

comes saturated above $\lambda = 4$. Because we expect that the degree of chain orientation is higher in the skin layer than the core, f of the skin and the core was also measured. The skin samples have a thickness of 0.2 mm and the core samples have a circular cross section with a radius equal to 45% of that of the extruded rods (i.e., the core samples have a cross-sectional area equal to about 20% of that of the extruded rods). The degree of orientation in the core sample should be quite uniform because reducing its radius by a factor of 2 gives essentially the same f value.

It is seen from Figure 1 that f in the skin layer has a high value of about 0.88 even at a low draw ratio of 1.3, and this value remains unchanged up to $\lambda = 15$. In contrast, f in the core increases from 0.15 to 0.86 as λ increases from 1.3 to 4.6, above which its value becomes saturated. As expected, the f values for the extruded rods fall between those for the skin and core samples. At $\lambda \geq 4.6$, the f values for the skin, core, and whole rod are the same within experimental accuracy. The skin–core structure is directly related to the velocity profile at the exit of the die.[14] The skin comes from oriented fluid elements that have been stretched whereas the core comes from fluid elements that have been axially compressed due to deceleration. As the draw ratio increases the extent of the skin region increases until finally the whole rod has a high degree of orientation at $\lambda > 4$.

Thermal Conductivity

The thermal conductivities of the extruded rods of Vectra B950 parallel ($K_{\parallel}$) and perpendicular ($K_{\perp}$) to the draw direction are shown as functions of λ in Figure 2. The axial thermal conductivity $K_{\parallel}$ rises sharply at low λ but becomes saturated at $\lambda > 4$, whereas the transverse thermal conductivity shows the opposite trend. The changes in $K_{\parallel}$ and $K_{\perp}$ can be attributed to the rapid increase in chain alignment shown in Figure 1. Above $\lambda = 4$, f has a constant value, so there is very little change in $K_{\parallel}$ or $K_{\perp}$. As shown in Figure 2, the $K_{\parallel}$ and $K_{\perp}$ values for a Vectra A950 rod at $\lambda = 3$ are close to those for Vectra B950, implying that the thermal conductivity is not very sensitive to chemical composition.

At $\lambda < 2$, the $K_{\parallel}$ values for the rods are 10–15% higher than those for the core samples, but they agree to within the experimental accuracy (6%) at higher λ. The difference in $K_{\parallel}$ at low λ can be accounted for if we assume that the skin region in these rod samples has an axial thermal conductivity similar to that of the highly oriented rod.

In Figure 3, the draw ratio dependence of $K_{\parallel}$ for Vectra B950 is compared with those for several flexible chain polymers[15–17] that have been drawn from the solid state. Because of the sharp rise in $K_{\parallel}$ at low λ, the TLCP has the highest $K_{\parallel}$ below $\lambda = 3$. However, $K_{\parallel}$ of the TLCP reaches a plateau at $\lambda > 4$, so its value at high λ is only slightly higher than that of polypropylene (PP) but significantly lower than those of polyethylene (PE) and polyoxymethylene (POM). Although the chains in the crys-

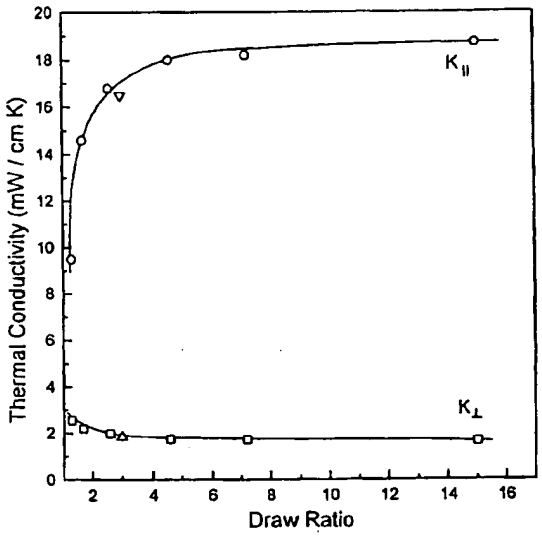

Figure 2. Draw ratio dependence of the axial ($K_{\parallel}$) and transverse ($K_{\perp}$) thermal conductivity of Vectra B950 at 300 K. $K_{\parallel}$ (▽) and $K_{\perp}$ (△) data for Vectra A950 are included.

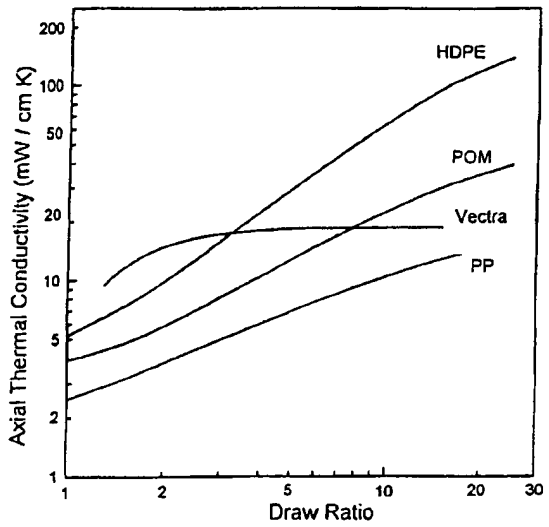

Figure 3. Draw ratio dependence of the axial thermal conductivity of Vectra B950, high-density polyethylene (HDPE), polyoxymethylene (POM), and polypropylene (PP) at 300 K. Data for HDPE, POM, and PP are taken from ref. 15, 16, and 17, respectively.

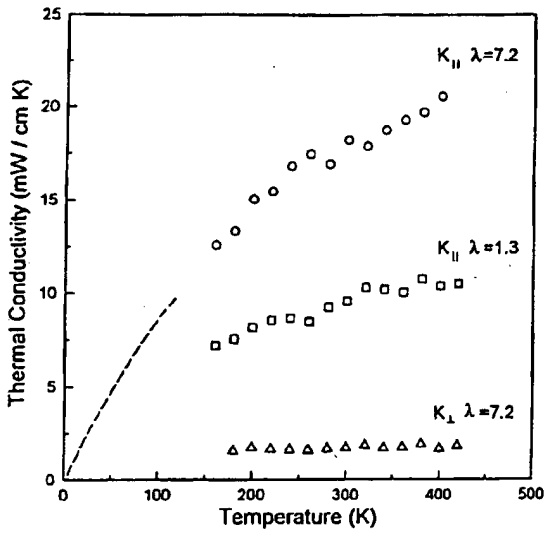

Figure 4. Temperature dependence of the axial ($K_{\|}$) and transverse ($K_{\perp}$) thermal conductivity of Vectra B950. The dashed line denotes $K_{\|}$ data for highly oriented HNA/HBA copolyesters taken from ref. 7.

talline phase of these flexible chain polymers are mostly aligned at a low draw ratio ($\lambda = 4$), the degree of chain orientation in the amorphous regions and the number of taut tie molecules increase steadily up to the highest achievable draw ratio,[17,18] and this causes the continued rise in $K_{\|}$. In contrast, the semirigid molecules in the localized domains of the nematic melt of a TLCP have parallel orientation, so the elongational stress during drawing readily induces the molecules to align along the draw direction. This leads to the saturation in both f and $K_{\|}$ at $\lambda > 4$.

The temperature dependencies of $K_{\|}$ and $K_{\perp}$ of Vectra B950 are shown in Figure 4. It is clear that $K_{\|}$ rises appreciably with temperature whereas $K_{\perp}$ is almost independent of temperature. The stronger temperature dependence for $K_{\|}$ arises from the fact that $K_{\|}$ is largely contributed by intrachain vibrations that have a high Debye temperature. On the other hand, the interchain vibrations have a low Debye temperature and thus leads to a $K_{\perp}$ that is independent of temperature. Crispin and Greig[7] have studied the thermal conductivity of HNA/HBA copolyesters below 100 K and have found that $K_{\|}$ is independent of composition for HNA content varying from 25 to 70 mol %. It is seen from Figure 4 that our data extrapolate smoothly to the curve obtained by Crispin and Greig. Because our TLCP sample contains 58 mol % HNA, 21 mol % terephthalic acid, and 21 mol % para-aminophenol, the result further confirms that the thermal conductivity of this class of TLCP is not very sensitive to variation in chemical composition.

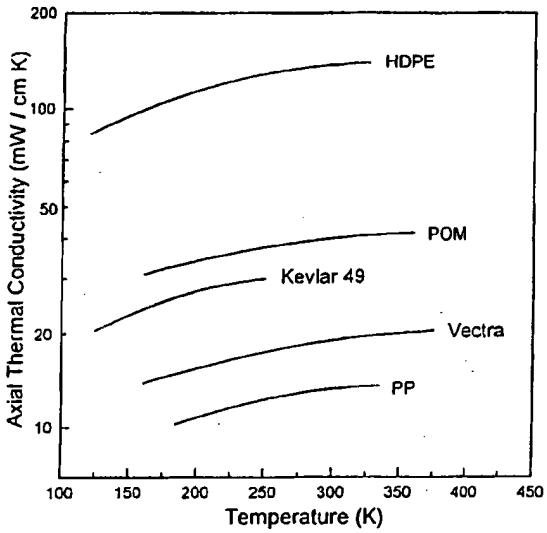

Figure 5. Temperature dependence of the axial thermal conductivity of Vectra B950 ($\lambda = 15$), Kevlar 49, high-density polyethylene (HDPE, $\lambda = 25$), polyoxymethylene (POM, $\lambda = 26$), and polypropylene (PP, $\lambda = 17$). Data for Kevlar 49, HDPE, POM, and PP are taken from ref. 19, 15, 16, and 17, respectively.

Figure 5 shows a comparison of the axial thermal conductivity of Vectra B950, a lyotropic LCP, poly(*p*-phenylene terephthalamide) (Kevlar 49),[19] and three flexible chain polymers.[15-17] The magnitude of $K_{||}$ for the flexible chain polymers covers a wide range, with the $K_{||}$ value for PE at $\lambda = 25$ being one order of magnitude higher than that of PP at $\lambda = 17$. In fact, the range is even wider if we include the data for gel-spun PE fibers.[20] Because of the reduced chain entanglement, gel PE samples can be drawn to $\lambda > 100$, thereby giving a $K_{||}$ that is about three times the value shown in Figure 5. The high thermal conductivity of oriented PE arises from the large fraction of highly thermally conducting extended chain crystals connecting the folded chain crystalline blocks.[20]

It is also seen from Figure 5 that the thermal conductivities of Kevlar 49 and Vectra B950 are higher than that of PP but much lower than that of PE. The thermal conduction mechanisms in LCP are not known but it is safe to assume that their relatively low thermal conductivity compared to PE results from the more complicated chemical structure of the polymer chains. For Kevlar 49, the chain backbone consists of phenyl groups as well as carbon and nitrogen atoms, whereas for Vectra B950 the three different monomers are randomly distributed along the chain.

Because both $K_{||}$ and the axial Young's modulus $E_{||}$[18,21-23] are primarily controlled by chain orientation, a relationship should exist between these two quantities. A roughly linear relation was found for PE,[15] and this is shown in Figure 6, together with the corresponding curves for POM, PP, and the TLCP. It is obvious that the slopes of the curves are different for different materials, with the slope for PE being much steeper than that for the TLCP. As a result, for a sevenfold increase in $E_{||}$, $K_{||}$ of PE and the TLCP increases by factors of 7 and 2, respectively. Therefore, highly oriented PE has both high stiffness and high thermal conductivity whereas the TLCP has high stiffness but only moderate thermal conductivity.

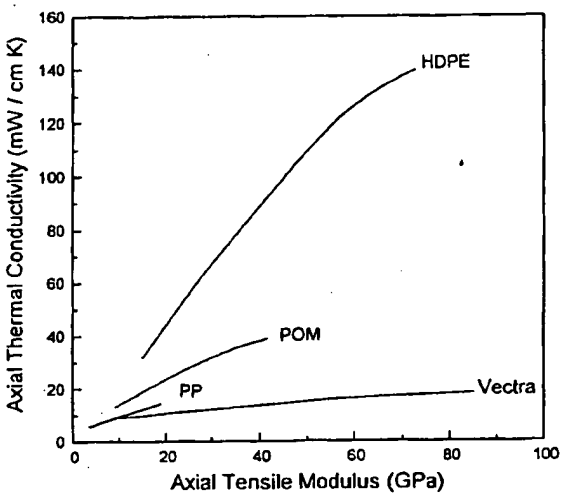

Figure 6. Variation of the axial thermal conductivity with the axial tensile modulus for several polymers at 300 K. The tensile modulus data for Vectra B950, HDPE, POM, and PP are taken from ref. 21, 22, 23, and 18, respectively.

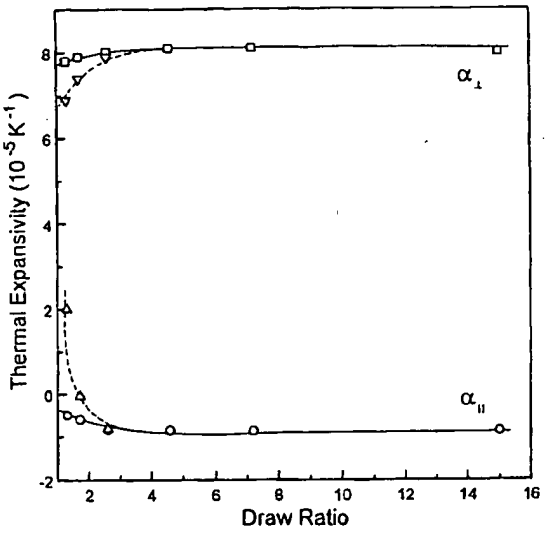

Figure 7. Draw ratio dependence of the axial ($\alpha_{||}$) and transverse ($\alpha_\perp$) thermal expansivity of Vectra B950 at 300 K. $\alpha_{||}$: rod, O; core, Δ. $\alpha_\perp$: rod, □; core, ▽.

Thermal Expansivity

The thermal expansivities of the rod and core samples of Vectra B950 parallel and perpendicular to the draw direction are shown in Figure 7. The axial thermal expansivity $\alpha_{||}$ drops sharply with increasing draw ratio whereas the transverse expansivity $\alpha_\perp$ shows a slight increase. The saturation effect for the thermal expansivity occurs at a lower λ than the thermal conductivity, with $\alpha_{||}$ and $\alpha_\perp$ having constant values of about -0.85×10^{-5} and 8.0×10^{-5} K^{-1} above $\lambda = 2.6$. It is seen from Figure 7 that at $\lambda < 2$ $\alpha_{||}$ for the rod is much lower than that for the core. This is because the skin layer not only has a negative $\alpha_{||}$ but also a high axial stiffness, thus constraining the axial expansion of the core region in the rod.

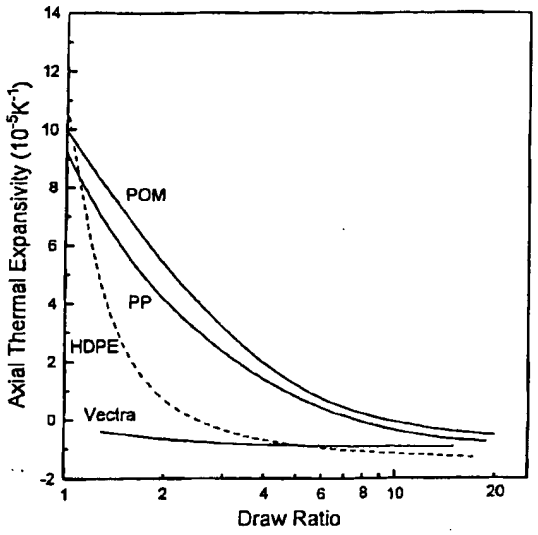

Figure 8. Draw ratio dependence of the axial thermal expansivity of Vectra B950, high-density polyethylene (HDPE), polyoxymethylene (POM), and polypropylene (PP) at 300 K. The data for HDPE, POM, and PP are taken from ref. 13 and 24.

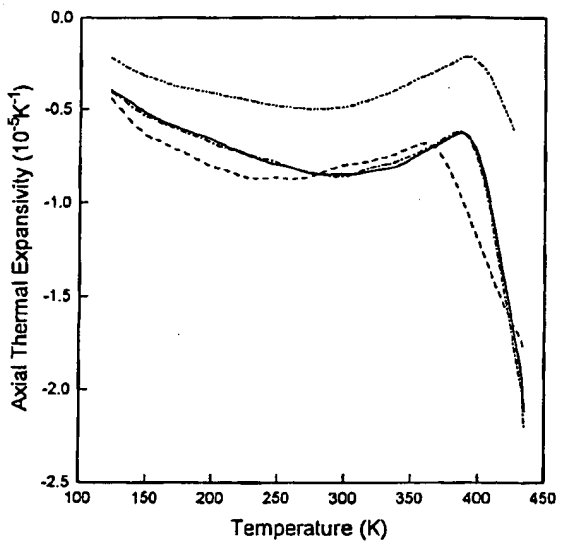

Figure 9. Temperature dependence of the axial thermal expansivity of extruded liquid crystalline polymers. Vectra B950: — · · λ = 1.3, — λ = 4.6, - · - · λ = 15. Vectra A950: --- λ = 3.

Figure 8 shows a comparison of the draw ratio dependence of $\alpha_{\parallel}$ for Vectra B950 and three flexible chain polymers, PE, POM, and PP.[13,24] The effect of drawing is so strong for Vectra B950 that $\alpha_{\parallel}$ has become negative at a low draw ratio of 1.3. The axial thermal expansivity for the flexible chain polymers also decreases with increasing λ, with $\alpha_{\parallel}$ becoming negative at λ = 3 for PE and at λ = 7 for POM and PP. It is interesting to note that at high λ $\alpha_{\parallel}$ for all four polymers not only has the same sign but also a similar magnitude. This points to a universal mechanism that will be discussed further when we consider the temperature dependence of $\alpha_{\parallel}$.

The temperature dependences of $\alpha_{\parallel}$ and $\alpha_{\perp}$ of the extruded rods of Vectra B950 are shown in Figures 9 and 10, respectively. Because the temperature dependence is similar for different draw ratios, only the curves at a few λ values are shown. It is seen from Figure 9 that $\alpha_{\parallel}$ decreases as the temperature increases from 120 to 270 K. Near this temperature, the slope of the curves changes from negative to positive, indicating the possible existence of a transition. A more pronounced transition occurs at about 390 K, above which $\alpha_{\parallel}$ exhibits a sharp drop. Figure 10 reveals that changes in slope are also observed for $\alpha_{\perp}$ in the two transition regions. The strong transition at about 390 K is associated with large-scale segmental motions of the polymer chains and is notionally similar to the glass transition of conventional polymers. Such a transition is also found in dynamic mechanical experiments and is labeled the α relaxation.[25] The weaker β transition at about 270 K has also been detected and attributed to the local motion of the naphthalene units.[25]

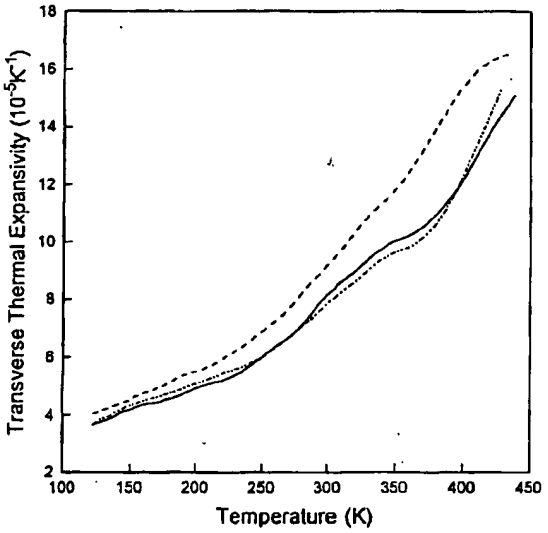

Figure 10. Temperature dependence of the transverse thermal expansivity of extruded liquid crystalline polymers. Vectra B950: — · · λ = 1.3, — λ = 4.6. Vectra A950: --- λ = 3.

Even though Vectra B950 and Vectra A950 have different chemical composition, the thermal expansivity of the highly oriented samples ($\lambda \geq 3$) has similar magnitude and temperature dependence (see Figs. 9 and 10). However, the high-temperature transition in Vectra B950 occurs at 25 K higher, reflecting the higher glass transition temperature of this material.[6,25] Moreover, $\alpha_\perp$ for Vectra B950 is lower by 10–20%, which arises from the stronger interchain interaction due to the presence of hydrogen bonds.

Figure 11 shows that highly oriented samples of both flexible and rigid chain polymers[26] exhibit negative thermal expansion along the draw direction. The physical origin of this universal phenomenon is now understood.[24,27,28] As a result of the strong anisotropy in the interaction forces, the torsional and bending motions of the chains are more highly excited than the stretching modes, and this leads to an effective shortening of the interatomic distance along the chain direction. A detailed calculation on polyethylene crystal[27] shows that torsional vibrations give a contribution of about 60% and the resulting room temperature axial expansivity of -1.3×10^{-5} K^{-1} is in excellent agreement with the observed value.[29] It is seen from Figure 11 that $\alpha_\parallel$ for highly oriented PE is only 10% higher than the axial expansivity of PE crystal because the extended chain crystals in the microfibrils have extremely high stiffness and thus strongly constrain the expansion of the adjacent amorphous regions.[13,24] The fact that LCP and flexible chain polymers have similar $\alpha_\parallel$ values below the glass transition temperature imply that the same microscopic mechanism is involved.

Above the glass transition temperature, however, an additional mechanism may come into play.[24] Most, if not all, of the tie molecules in POM and PP have an amorphous nature,[23] and the tendency to assume a more crumpled conformation leads to a sharp drop in $\alpha_\parallel$ (entropic contraction). This effect is also observed in Vectra, indicating that the tie molecules between the crystalline lamellae in this class of TLCP possess considerable semiflexibility. This is consistent with the observations of disinclination morphologies, which show that the splay elastic constant is greater than the bend elastic constant.[30]

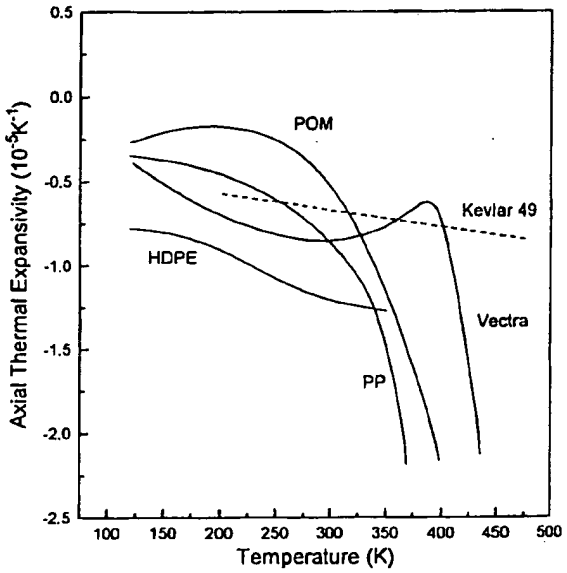

Figure 11. Temperature dependence of the axial thermal expansivity of Vectra B950 ($\lambda = 4.6$), Kevlar 49, high-density polyethylene (HDPE, $\lambda = 18$), polyoxymethylene (POM, $\lambda = 20$), and polypropylene (PP, $\lambda = 18$). Data for Kevlar 49 are taken from ref. 26 whereas data for HDPE, POM, and PP are taken from ref. 13 and 24.

Aggregate Model

The aggregate model[31-33] is commonly used to analyze the thermal conductivity and expansivity of flexible chain polymers, and this model has recently been applied to explain the thermal expansion behavior of TLCP.[10] In this model, an isotropic polymer is regarded as a random aggregate of axially symmetric units whose properties are those of the fully oriented materials. When the polymer is drawn, the intrinsic units rotate towards the draw direction, with the units themselves remaining unchanged. Then the thermal conductivity of a partially oriented sample can be calculated by using either the parallel or the series model. The parallel model assumes uniform temperature gradient throughout the aggregate, which implies a summation of the thermal conductivities, whereas the series model assumes uniform heat flux, thus leading to a summation of thermal resistivities. In the parallel model the thermal conductivities are given by:

$$K_\parallel = \tfrac{1}{3}[(1 + 2f)K^u_\parallel + 2(1 - f)K^u_\perp] \quad (1)$$

$$K_\perp = \tfrac{1}{3}[(1 - f)K^u_\parallel + (2 + f)K^u_\perp] \quad (2)$$

where $K^u_\parallel$ and $K^u_\perp$ are the thermal conductivities of the intrinsic unit. For the isotropic material $f = 0$, so it follows from eqs. (1) and (2) that

$$K_{iso} = \tfrac{1}{3}(K_\parallel + 2K_\perp) \quad (3)$$

$$= \tfrac{1}{3}(K^u_\parallel + 2K^u_\perp). \quad (4)$$

Table I. Thermal Conductivity and Thermal Expansivity of Isotropic Vectra B950 Predicted by the Aggregate Model

	Draw Ratio	1.3	1.7	2.6	4.6	7.2	15
Parallel model	K^P_{iso} (mW/cm K)	4.87	6.33	6.93	7.16	7.21	7.34
Series model	K^S_{iso} (mW/cm K)	3.38	3.07	2.82	2.49	2.46	2.38
Series model	α^S_{iso} (10^{-5} K^{-1})	5.04	5.07	5.06	5.12	5.11	5.05

Expression for the series model can be obtained simply by replacing all the K in eqs. (1)–(4) by K^{-1}.

The parallel and series models provide upper and lower theoretical bounds for the thermal conductivity, so a comparison with the observed values will show which model more closely resembles the actual situation. The models can be applied in two ways. First, using the observed thermal conductivities at any draw ratio, we can calculate the thermal conductivity of isotropic Vectra B950, K^P_{iso} or K^S_{iso}, according to the parallel or series model (Table I). We have not prepared undrawn rods of Vectra B950 but measurement on the core of an undrawn rod of Vectra 900 (a TLCP of almost identical chemical composition)[3] gives a thermal conductivity of 4.9 mW/cm K, which is taken as K_{iso} for Vectra B950. It is seen from Table I that the theoretical values K^P_{iso} and K^S_{iso} varies with increasing λ and this disagrees with eq. (4), which predicts an isotropic thermal conductivity independent of λ. The observed K_{iso} of 4.9 mW/cm K lies between the bounds, but is closer to the upper bound predicted by the parallel model.

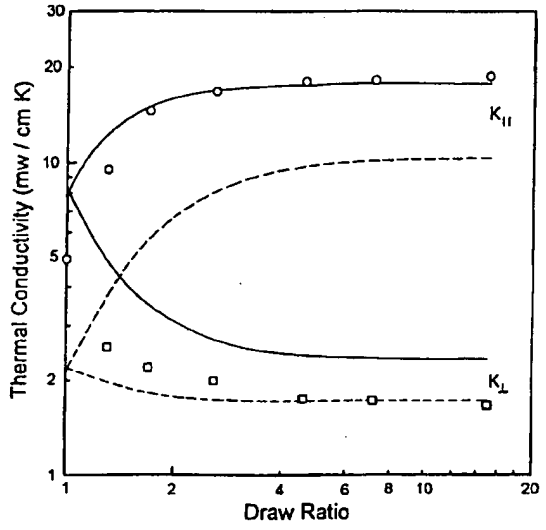

Figure 12. Comparison of the observed axial ($K_{||}$) and transverse ($K_\perp$) thermal conductivity of Vectra B950 with predictions of the aggregate model. The solid and dashed lines are the predictions of the parallel and series model, respectively. The data point at draw ratio = 1 is for Vectra B900.

The pattern of anisotropy of the thermal conductivity can also be predicted if the thermal conductivities of the intrinsic units are known. By fitting the thermal conductivities at high λ to a polynomial a + b/λ and extrapolating to λ = ∞, we obtain $K^u_{||}$ = 19 mW/cm K and $K^u_\perp$ = 1.65 mW/cm K. Using these values, $K_{||}$ and $K_\perp$ are calculated as functions of λ and are shown in Figure 12. It is clear that there is agreement between theory and experiment in the general trends of the draw ratio dependence, namely, the sharp rise in $K_{||}$ and the moderate fall in $K_\perp$. However, the $K_{||}$ data follow closely the upper bound whereas the $K_\perp$ data lie between the two bounds.

A similar application of the series model to the thermal expansivity gives:

$$\alpha_{||} = \tfrac{1}{3}[(1 + 2f)\alpha^u_{||} + 2(1 - f)\alpha^u_\perp] \quad (5)$$

$$\alpha_\perp = \tfrac{1}{3}[(1 - f)\alpha^u_{||} + (2 + f)\alpha^u_\perp] \quad (6)$$

$$\alpha_{iso} = \tfrac{1}{3}(\alpha_{||} + 2\alpha_\perp) \quad (7)$$

$$= \tfrac{1}{3}(\alpha^u_{||} + 2\alpha^u_\perp). \quad (8)$$

It is seen from Table I that the predicted α^S_{iso} based on eq. (7) is roughly independent of λ and is only about 15% lower than the value of 5.8×10^{-5} K^{-1} obtained for isotropic Vectra B900. Using $\alpha^u_{||} = -0.85 \times 10^{-5}$ K^{-1} and $\alpha^u_\perp = 8 \times 10^{-5}$ K^{-1} the draw ratio dependence is calculated and shown in Figure 13. Although the sharp fall in $\alpha_{||}$ and the slight rise in $\alpha_\perp$ are correctly predicted, the theoretical values for $\alpha_{||}$ drop more slowly than the experimental data.

It is not appropriate to simply replace all the α in eqs. (5)–(8) by α^{-1} to obtain expressions for the parallel model. Because $\alpha^u_{||}$ and $\alpha^u_\perp$ have opposite signs, this would give an infinite value for $\alpha_\perp$ at a certain draw ratio, which is obviously unphysical. Therefore, a more refined treatment is required for

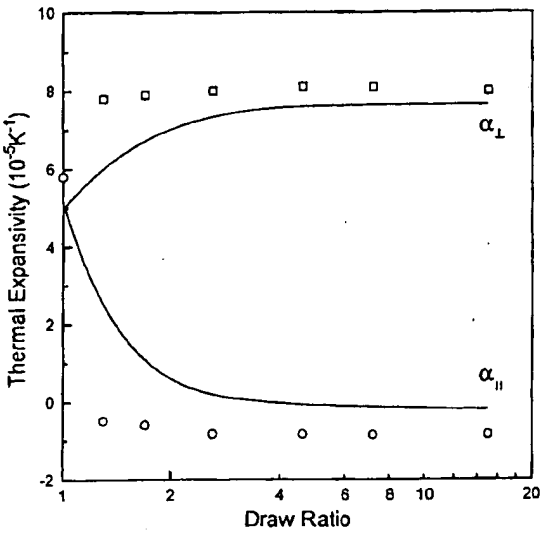

Figure 13. Comparison of the observed axial ($\alpha_\parallel$) and transverse ($\alpha_\perp$) thermal expansivity of Vectra B950 with predictions of the series model. The solid lines are the predictions. The data point at draw ratio = 1 is for Vectra B900.

the case where the intrinsic units are arranged in parallel.

CONCLUSION

The sharp rise in the axial thermal conductivity and the drastic drop in the axial expansivity of Vectra B950 at low draw ratio, and the saturation of these two quantities at $\lambda > 4$ reflect the corresponding increase in the degree of chain alignment. In the transverse direction, the thermal conductivity and expansivity exhibit the opposite trends but the changes are relatively small. The pattern of anisotropy of the thermal conductivity agrees reasonably with the predictions of both the parallel and series model. However, $K_\parallel$ follows closely the upper bound predicted by the parallel model, whereas $K_\perp$ lies between the two bounds. Although the draw ratio dependence of the thermal expansivity is reproduced by the series model, the observed $\alpha_\parallel$ drops more rapidly than the prediction. A comparison with the parallel model is not possible because the theoretical expressions based on this model are not yet available.

At high orientation, the axial thermal conductivity of Vectra B950 is slightly higher than that of polypropylene but one order of magnitude lower than that of polyethylene. Therefore, Vectra B950 is a polymer with very high elastic stiffness but only moderate thermal conductivity. Like flexible chain polymers, Vectra B950 has a negative axial expansivity, with a room temperature value differing from that of polyethylene by less than 50%. The negative expansion phenomenon, which arises from the effective shortening along the chain direction as a result of the bending and torsional motions of the chains, seems to be universal for both flexible and rigid chain polymers.

We are grateful to Dr. Q. Lin for preparing the B950 rods and to Dr. T. S. Chung of Hoechst-Celanese Co. for supplying the A950 rods. Thanks are also due to Mr. H. M. Ma for carrying out some of the thermal expansivity measurements.

REFERENCES AND NOTES

1. T. S. Chung, *J. Polym. Sci., Polym. Phys.*, **26**, 1549 (1988).
2. H. J. Zimmermann and J. H. Wendorff, *J. Mater. Sci.*, **23**, 2310 (1988).
3. C. L. Choy, W. P. Leung, and A. F. Yee, *Polymer*, **33**, 1788 (1992).
4. D. E. Turek and G. P. Simon, *Polymer*, **34**, 2763 (1993).
5. S. K. Garg and S. Kenig, in *High Modulus Polymers*, A. E. Zachariades and R. S. Porter (eds.), Marcel Dekker, New York, 1988.
6. G. R. Davies and I. M. Ward, in *High Modulus Polymers*, A. E. Zachariades and R. S. Porter (eds.), Marcel Dekker, New York, 1988.
7. A. J. Crispin and D. Greig, *Polym. Commun.*, **27**, 264 (1986).
8. C. L. Choy, W. P. Leung, and K. W. Kwok, *Polym. Commun.*, **32**, 285 (1991).
9. D. I. Green, G. A. J. Orchard, G. R. Davies, and I. M. Ward, *J. Polym. Sci., Polym. Phys.*, **28**, 2225 (1990).
10. Y. Takeuchi, F. Yamamoto, and Y. Shuto, *Macromolecules*, **19**, 2059 (1986).
11. R. A. Chivers and J. Blackwell, *Polymer*, **26**, 997 (1985).
12. C. L. Choy, W. P. Leung, and Y. K. Ng, *J. Polym. Sci., Polym. Phys.*, **25**, 1779 (1987).
13. C. L. Choy, F. C. Chen, and E. L. Ong, *Polymer*, **20**, 1191 (1979).
14. N. J. Alderman and M. R. Mackley, *Faraday Discuss., Chem. Soc.*, **79**, 149 (1985).
15. C. L. Choy, W. H. Luk, and F. C. Chen, *Polymer*, **19**, 155 (1978).
16. C. L. Choy, K. Nakagawa, and T. Konaka, unpublished.
17. C. L. Choy, F. C. Chen, and W. H. Luk, *J. Polym. Sci., Polym. Phys.*, **18**, 1187 (1980).

18. W. P. Leung and C. L. Choy, *J. Polym. Sci., Polym. Phys.*, **21**, 725 (1983).
19. B. Poulaert, J. C. Chielens, C. Vandenhende, and R. Legras, *Polym. Commun.*, **26**, 132 (1985).
20. C. L. Choy, Y. Fei, and T. G. Xi, *J. Polym. Sci., Polym. Phys.*, **31**, 365 (1993).
21. C. L. Choy, K. W. E. Lau, Y. W. Wong, and A. Y. Yee, *Polym. Eng. Sci.*, (in press).
22. C. L. Choy and W. P. Leung, *J. Polym. Sci., Polym. Phys.*, **23**, 1759 (1985).
23. W. P. Leung, C. L. Choy, K. Nakagawa, and T. Konaka, *J. Polym. Sci., Polym. Phys.*, **25**, 2059 (1987).
24. C. L. Choy, F. C. Chen, and K. Young, *J. Polym. Sci., Polym. Phys.*, **19**, 335 (1981).
25. H. Zhang, G. R. Davies, and I. M. Ward, *Polymer*, **33**, 2651 (1992).
26. T. Ii, K. Tashiro, M. Kobayashi, and H. Tadokoro, *Macromolecules*, **19**, 1809 (1986).
27. F. C. Chen, C. L. Choy, S. P. Wong, and K. Young, *J. Polym. Sci., Polym. Phys.*, **19**, 971 (1981).
28. C. L. Choy, S. P. Wong, and K. Young, *J. Polym. Sci., Polym. Phys.*, **22**, 979 (1984).
29. G. T. Davis, R. K. Eby, and J. P. Colson, *J. Appl. Phys.*, **41**, 4316 (1970).
30. S. D. Hudson and A. J. Lovinger, *Polymer*, **34**, 1123 (1993).
31. J. Hennig, *J. Polym. Sci. (C)*, **16**, 2751 (1967).
32. C. L. Choy, *Polymer*, **18**, 984 (1977).
33. C. L. Choy, in *Development of Oriented Polymers-1*, I. M. Ward (ed.), Applied Science Publishers, London, 1982, Chap. 4.

Received December 28, 1994
Revised March 27, 1995
Accepted April 6, 1995